

Tree-based Subgroup Discovery In Electronic Health Records: Heterogeneity of Treatment Effects for DTG-containing Therapies

Jiabei Yang^{*1}, Ann W. Mwangi²⁻³, Rami Kantor⁴, Issa J. Dahabreh⁵⁻⁷, Monicah Nyambura³,
Allison Delong¹, Joseph W. Hogan¹, and Jon A. Steingrimsson¹

¹Department of Biostatistics, School of Public Health, Brown University, Providence, RI

²Department of Mathematics, Physics & Computing, School of Science & Aerospace Studies, Moi University, Kenya

³Academic Model Providing Access to Healthcare (AMPATH), Kenya

⁴Division of Infectious Diseases, Warren Alpert Medical School, Brown University, Providence, RI

⁵CAUSALab, Harvard T.H. Chan School of Public Health, Boston, MA, Boston, MA

⁶Department of Epidemiology, Harvard T.H. Chan School of Public Health, Boston, MA

⁷Department of Biostatistics, Harvard T.H. Chan School of Public Health, Boston, MA

Wednesday 31st August, 2022

*Email: jiabei_yang@brown.edu.

Abstract: The rich longitudinal individual level data available from electronic health records (EHRs) can be used to examine treatment effect heterogeneity. However, estimating treatment effects using EHR data poses several challenges, including time-varying confounding, repeated and temporally non-aligned measurements of covariates, treatment assignments and outcomes, and loss-to-follow-up due to dropout. Here, we develop the Subgroup Discovery for Longitudinal Data (SDLD) algorithm, a tree-based algorithm for discovering subgroups with heterogeneous treatment effects using longitudinal data by combining the generalized interaction tree algorithm, a general data-driven method for subgroup discovery, with longitudinal targeted maximum likelihood estimation. We apply the algorithm to EHR data to discover subgroups of people living with human immunodeficiency virus (HIV) who are at higher risk of weight gain when receiving dolutegravir-containing antiretroviral therapies (ARTs) versus when receiving non dolutegravir-containing ARTs.

Key words: Causal Inference; Dolutegravir; Electronic health record; Heterogeneity of treatment effects; Longitudinal targeted maximum likelihood estimation; Machine learning; Recursive partitioning; Subgroup discovery.

1 Introduction

Dolutegravir (DTG) is an orally administered antiretroviral medication that in combination with other antiretroviral medications has been approved for the treatment of human immunodeficiency virus (HIV) infection [[World Health Organization, 2018](#)]. DTG-containing antiretroviral therapies (ARTs) have many advantages such as promising treatment efficacy, high medication resistance barrier and low cost compared with ARTs previously recommended by the World Health Organization (WHO) [[NAMSAL ANRS 12313 Study Group, 2019](#), [Phillips et al., 2019](#), [Venter et al., 2019](#)].

However, several randomized trials [Calmy et al., 2020, NAMSAL ANRS 12313 Study Group, 2019, Sax et al., 2020, Venter et al., 2019, 2020] and observational studies [Bourgi et al., 2020a,b, Esber et al., 2022, Surial et al., 2021] have found larger average weight gain among people receiving DTG-containing ARTs. Weight gains can have negative consequences among people living with HIV including increased risk of cardiovascular and metabolic diseases as well as other comorbidities [Achhra et al., 2016, Herrin et al., 2016, Kim et al., 2012]. A few studies have explored how weight gain differs between subgroups defined by some individual characteristics [Bourgi et al., 2020a, Calmy et al., 2020, Sax et al., 2020, Venter et al., 2020], but all of these studies focused on subgroups that were pre-specified by the investigators and did not attempt data-driven subgroup discovery.

Data-driven discovery of subgroups with heterogeneous treatment effects requires larger sample sizes than estimation of population average treatment effects [Dahabreh et al., 2016]. Unlike randomized controlled trials, which are usually powered to detect average treatment effects in the overall population, electronic health records (EHRs) often contain rich longitudinal data collected on a large number of diverse individuals in a “real world” setting. This makes EHRs well suited for more fine grained treatment effect analyses such as discovering subgroups with heterogeneous treatment effects and estimating long-term effects of sustained treatments. However, treatment effect estimation using EHRs involves several challenges including: i) EHRs have repeated measures over time, and these measures are not temporally aligned; ii) potential time-varying confounding; and iii) potentially informative dropout (i.e., individuals that dropout of the EHRs systematically differ from those who do not dropout).

Tree-based methods stratify the covariate space into interpretable subgroups making them ideal for subgroup discovery [Su et al., 2008]. In contrast, most other blackbox machine learning algorithms produce completely personalized predictions (rather than subgroup-specific predictions), and are therefore not applicable for subgroup discovery. Previous work on tree-based methods for discovering subgroups with differential treatment effects has mostly focused on cross-sectional randomized [Foster et al., 2011, Seibold et al., 2016, Steingrimsson and Yang, 2019, Su et al., 2009] or non-randomized data [Athey and Imbens, 2016, Yang et al., 2022]. Additionally, previ-

ously proposed tree-based methods for treatment effect estimation with longitudinal data [Su et al., 2011, Wei et al., 2020] cannot handle both non-randomized time-varying treatment assignment and dropout.

In this paper, we develop the first tree-based algorithm for discovering subgroups with heterogeneous treatment effects when comparing the effects of time-varying treatments using non-randomized longitudinal data, in the presence of potentially informative dropout (censoring). The algorithm we develop, referred to as the Subgroup Discovery for Longitudinal Data (SDL) algorithm, extends the generalized interaction tree algorithm [Yang et al., 2022] by combining it with longitudinal targeted maximum likelihood estimators (TMLE) [Petersen et al., 2014, Stitelman et al., 2012, van der Laan and Gruber, 2012, Van der Laan and Rose, 2018, Van der Laan et al., 2011, Van Der Laan and Rubin, 2006]. The SDL algorithm recursively splits the covariate space into disjoint subgroups using splitting decisions that are based on maximizing treatment effect heterogeneity as quantified by subgroup-specific TMLEs. TMLEs are doubly robust [Bang and Robins, 2005, Robins et al., 1994], semi-parametric efficient [Stitelman et al., 2012, Van der Laan and Rose, 2018], and guaranteed to take values in the support of the outcome. We apply the algorithm to perform the first data-driven discovery of subgroups with differential effect of DTG-containing ARTs on weight using EHRs of people living with HIV in western Kenya.

2 Data structure and target parameter

For $k \in \{0, \dots, K\}$, let \mathbf{L}_k be a vector of time-dependent covariates (that includes measures of the outcome Y_k) measured at time k , A_k be the binary treatment indicator at time k , C_k be an indicator whether a person drops out at time k , and Y_{K+1} be the outcome at time $K + 1$. The baseline covariates \mathbf{L}_0 can include covariates that do not vary over time and baseline values of time-varying covariates. We assume the following time ordering of the data

$$\mathbf{O} = (\mathbf{L}_0, A_0, C_0, \mathbf{L}_1, A_1, C_1, \dots, \mathbf{L}_K, A_K, C_K, Y_{K+1}).$$

By the time ordering assumption, each variable has no causal effect on those measured before. For a vector $\mathbf{X} = (X_0, \dots, X_K)$, define $\overline{\mathbf{X}}_k = (X_0, \dots, X_k)$, $\underline{\mathbf{X}}_k = (X_{k+1}, \dots, X_K)$, and \mathbf{X} without subscript indicates a vector from time 0 to K (i.e., $\mathbf{X} = \overline{\mathbf{X}}_K$). We assume that if an individual drops out at time k , all quantities measured after time k are not observed. That is, $C_k = 1$ implies that $\underline{\mathbf{C}}_k$, $\underline{\mathbf{L}}_k$, $\underline{\mathbf{A}}_k$, and Y_{K+1} are not observed.

Let $\overline{\mathbf{Y}}_{K+1,i}^{\mathbf{a},c=0}$ be the vector of potential outcomes [Rubin, 1974, Robins and Greenland, 2000] under intervention on individual i to set the treatment vector \mathbf{A}_i to \mathbf{a} and to abolish censoring (i.e., intervention to set $\mathbf{C}_i = \mathbf{0}$). Similarly, let $\overline{\mathbf{L}}_{K,i}^{\mathbf{a},c=0}$ be the potential covariate trajectory of the i th individual under intervention to set the treatment vector \mathbf{A}_i to \mathbf{a} and to abolish censoring.

Let \mathbf{L}_0 take values in \mathcal{L}_0 . Any set $w \subseteq \mathcal{L}_0$ defines a subgroup consisting of individuals with $\mathbf{L}_0 \in w$. Define the treatment effect contrasting treatment regimes \mathbf{a}_1 and \mathbf{a}_0 within subgroup w as $\delta(w) = \text{E}[Y_{K+1}^{\mathbf{a}_1,c=0} | \mathbf{L}_0 \in w] - \text{E}[Y_{K+1}^{\mathbf{a}_0,c=0} | \mathbf{L}_0 \in w]$. That is, $\delta(w)$ is the subgroup-specific average treatment effect contrasting the treatment regimes \mathbf{a}_1 and \mathbf{a}_0 . Our objective is to find mutually exclusive and exhaustive subgroups of \mathcal{L}_0 where splitting decisions are made to maximize the between subgroup treatment effect difference.

3 Subgroup Discovery for Longitudinal Data (SDLD) algorithm

3.1 Generalized interaction tree algorithm

In this section, we briefly review the generalized interaction tree algorithm that has been used to discover subgroups with heterogeneous treatment effects for cross-sectional randomized trial data [Su et al., 2009, Steingrimsson and Yang, 2019] and cross-sectional observational data [Yang et al., 2022].

The generalized interaction tree algorithm consists of three steps: initial tree building, pruning, and final tree selection. The algorithm starts by splitting the data into an initial tree building dataset and a validation dataset. Algorithm 1 describes the initial tree building process that runs on the initial tree building dataset where the generalized interaction tree algorithm recursively partitions the covariate space into subgroups until a pre-determined stopping criterion is met

(e.g., there are too few observations in each subgroup to justify further splitting). At each attempt to partition the covariate space, the algorithm focuses on discovering subgroups that maximize differences between subgroup-specific treatment effect estimators (using some estimator, $\widehat{\delta}(w)$, of the treatment effect in subgroup w). In Section 3.2 we describe three subgroup-specific treatment effect estimators appropriate for the longitudinal data structures presented in Section 2. For a given subgroup-specific treatment effect estimator $\widehat{\delta}(w)$, define the splitting criterion for splitting a subgroup (node) w into two exclusive and exhaustive subgroups l and r as

$$\left(\frac{\widehat{\delta}(l) - \widehat{\delta}(r)}{\sqrt{\widehat{\text{Var}}[\widehat{\delta}(l) - \widehat{\delta}(r)]}} \right)^2. \quad (1)$$

The splitting criterion (1) estimates a standardized difference between the treatment effects in the two subgroups l and r . Selecting the subgroups l and r by maximizing the splitting criterion (1) results in a split that tries to find the pair of subgroups that have the largest difference in estimated treatment effects (i.e., maximizing estimated between subgroup treatment effect heterogeneity).

Algorithm 1 Initial tree building process for the SDL D algorithm

- 1: Define the root node as consisting of all observations. Set the root node as the node under consideration.
 - 2: Define $L_0^{(j)}$ as the j -th component of the baseline covariate vector. In the node under consideration, find all permissible $(L_0^{(j)}, c)$ pairs, $j = 1, \dots, J$, that split the covariate space into two groups defined by $l = \{L_0^{(j)} < c\}$ and $r = \{L_0^{(j)} \geq c\}$, where J is the number of components in the baseline covariate vector.
 - 3: Run through all possible splits in Step 2 and split the node under consideration into two new subgroups based on the split that maximizes the splitting criterion (1).
 - 4: If a pre-determined stopping criterion is met, stop the tree building process; otherwise, on every node that is not already split and has not met the stopping criterion, repeat Steps 2-4.
-

We refer to the result of Algorithm 1 as the initial tree $\widehat{\psi}_{\max}$. The initial tree $\widehat{\psi}_{\max}$ usually substantially overfits to the data and to reduce overfitting a pruning algorithm uses the initial tree building dataset to create a set of subtrees of $\widehat{\psi}_{\max}$ that are candidates for being the final tree (i.e., the final model). The pruning algorithm is described in detail in Appendix A. In short, the

pruning algorithm is based on the split complexity, which for a tree ψ is defined as

$$G^\lambda(\psi) = \sum_{w \in W_\psi} G_w(\psi) - \lambda |W_\psi|, \quad (2)$$

where W_ψ is the set of internal nodes, $G_i(\psi)$ is the value of the splitting criterion for internal node w , $|S_\psi|$ is the number of internal nodes, and λ is a positive penalization parameter. The first term in equation (2) is a measure of the treatment effect heterogeneity of the tree and each additional split in the tree is guaranteed to increase (or at least not decrease) the first term. To offset that, the second term penalizes the size of the tree (a measure of the complexity of the model). For a fixed λ , a subtree of the initial tree is said to be an optimal subtree if it maximizes $G^\lambda(\psi)$. Varying λ from 0 to ∞ results in a sequence of subtrees of different sizes, $\hat{\psi}_0 = \hat{\psi}_{\max}, \hat{\psi}_1, \dots, \hat{\psi}_{\hat{D}}$, that all are optimal for different intervals of λ .

In the original classification and regression tree algorithm for outcome prediction [Breiman et al., 1984], the final tree from the sequence of trees created by the pruning algorithm is selected by optimizing a cross-validated objective function. However, as the true treatment effect is unknown for all individuals (we only observe at most one of the potential outcomes $Y_{K+1,i}^{a_1, c=0}$ or $Y_{K+1,i}^{a_0, c=0}$), there is no observed treatment effect for each individual to compare the treatment effect predictions to in the cross-validation procedure. Hence, cross-validation cannot be applied directly to select the final tree in the generalized interaction tree algorithm. To overcome that, the generalized interaction tree algorithm selects the final tree by estimating the split complexity on the validation dataset. For a given tree $\hat{\psi}_d$ ($d \in \{0, 1, \dots, \hat{D}\}$) and a fixed λ , we calculate the validation split complexity by recalculating the split complexity in equation (2) using the validation dataset. The final tree is selected as the tree that maximizes the validation split complexity. This relies on specifying a value of λ and a common choice is to use a quantile (e.g., the 95th) of the χ_1^2 distribution [Steingrímsson and Yang, 2019, Su et al., 2008, Yang et al., 2022], which is the asymptotic distribution of the splitting criterion (1) when there is no treatment effect heterogeneity.

By implementing the initial tree building, pruning, and final tree selection, the generalized interaction tree algorithm stratifies the covariate space \mathcal{L}_0 into mutually exclusive and exhaustive

subgroups $\widehat{w}_1, \dots, \widehat{w}_{\widehat{M}}$ (terminal nodes).

3.2 Subgroup-specific treatment effect estimation

Implementation of the generalized interaction tree algorithm relies on estimating the subgroup-specific treatment effect $\delta(w) = \text{E}[Y_{K+1}^{\mathbf{a}_1, \mathbf{c}=\mathbf{0}} | \mathbf{L}_0 \in w] - \text{E}[Y_{K+1}^{\mathbf{a}_0, \mathbf{c}=\mathbf{0}} | \mathbf{L}_0 \in w]$. In this section, we describe how TMLE can be used to estimate $\text{E}[Y_{K+1}^{\mathbf{a}, \mathbf{c}=\mathbf{0}} | \mathbf{L}_0 \in w]$ for a treatment regime \mathbf{a} .

3.2.1 Identifiability

The following identifiability assumptions are needed for the potential outcome mean $\text{E}[Y_{K+1}^{\mathbf{a}, \mathbf{c}=\mathbf{0}} | \mathbf{L}_0 \in w]$ to be identifiable [Robins, 1986, Pearl and Robins, 1995, Bang and Robins, 2005]:

- Consistency: For time k , $k \in \{0, \dots, K\}$, and for every individual receiving treatment $\overline{\mathbf{A}}_k = \overline{\mathbf{a}}_k$ that has not dropped out of the study, their observed outcome at time $k + 1$ (Y_{k+1}) is equal to their potential outcome $Y_{k+1}^{\overline{\mathbf{a}}_k, \overline{\mathbf{c}}_k=\mathbf{0}}$ and their observed covariate trajectory is equal to their potential covariate trajectory.
- Sequential exchangeability: At time k , $k \in \{0, \dots, K\}$, the potential outcomes $(Y_{k+1}^{\overline{\mathbf{a}}_k, \overline{\mathbf{c}}_k}, \dots, Y_{K+1}^{\mathbf{a}, \mathbf{c}})$ are independent of treatment A_k and censoring status C_k conditional on past treatment and covariate trajectories.
- Positivity: For time k , $k \in \{0, \dots, K\}$, and all $\overline{\mathbf{l}}_k$ such that the density $f(\overline{\mathbf{L}}_k = \overline{\mathbf{l}}_k, \overline{\mathbf{A}}_{k-1} = \overline{\mathbf{a}}_{k-1}, \overline{\mathbf{C}}_{k-1} = \mathbf{0}) > 0$,

$$\Pr(A_k = a_k | \overline{\mathbf{L}}_k = \overline{\mathbf{l}}_k, \overline{\mathbf{A}}_{k-1} = \overline{\mathbf{a}}_{k-1}, \overline{\mathbf{C}}_{k-1} = \mathbf{0}) > 0,$$

where $\overline{\mathbf{A}}_{-1}$ is defined as the empty set and $\overline{\mathbf{C}}_{-1} = \mathbf{0}$. The positivity assumption says that conditional on past treatment and covariate history there is a positive probability of continuing to follow the treatment regime of interest.

Using these assumptions, the potential outcome mean can be written as

$$\mathbb{E} \left[\frac{I(\mathbf{A} = \mathbf{a}, \mathbf{C} = \mathbf{0})}{P(\mathbf{A} = \mathbf{a}, \mathbf{C} = \mathbf{0} | \mathbf{L})} Y_{K+1} \middle| \mathbf{L}_0 \in w \right] / \mathbb{E} \left[\frac{I(\mathbf{A} = \mathbf{a}, \mathbf{C} = \mathbf{0})}{P(\mathbf{A} = \mathbf{a}, \mathbf{C} = \mathbf{0} | \mathbf{L})} \middle| \mathbf{L}_0 \in w \right] \quad (3)$$

or as a series of iterated conditional expectations [Robins, 1986]

$$\mathbb{E}[Y_{K+1}^{\mathbf{a}, \mathbf{c}=\mathbf{0}} | \mathbf{L}_0 \in w] = \mathbb{E}[\mathbb{E}[\dots \mathbb{E}[Y_{K+1} | \mathbf{L}, \mathbf{A} = \mathbf{a}, \mathbf{C} = \mathbf{0}] \dots | \mathbf{L}_0, A_0 = a_0, C_0 = 0] | \mathbf{L}_0 \in w]. \quad (4)$$

3.2.2 Estimation

Before describing the longitudinal TMLE we start by describing inverse probability weighting (IPW) [Robins and Rotnitzky, 1992] and g-computation estimators [Robins, 1986] that are sample analogs of expressions (3) and (4), respectively. Denote the probability of following the treatment regime of interest at time k , $k \in \{0, \dots, K\}$, conditional on observed treatment and covariate history and not having dropped out from the study as

$$g_{A,k}(\bar{\mathbf{L}}_k, \bar{\mathbf{A}}_{k-1}; \bar{\mathbf{C}}_{k-1} = \mathbf{0}) = \Pr(A_k = a_k | \bar{\mathbf{L}}_k, \bar{\mathbf{A}}_{k-1}, \bar{\mathbf{C}}_{k-1} = \mathbf{0}).$$

Similarly, denote the probability of not dropping out from the study at time k , $k \in \{k = 0, \dots, K\}$, conditional on observed treatment and covariate history as

$$g_{C,k}(\bar{\mathbf{L}}_k, \bar{\mathbf{A}}_k; \bar{\mathbf{C}}_{k-1} = \mathbf{0}) = \Pr(C_k = 0 | \bar{\mathbf{L}}_k, \bar{\mathbf{A}}_k, \bar{\mathbf{C}}_{k-1} = \mathbf{0}).$$

For simplicity of notation, denote $g_{A,k}(\bar{\mathbf{L}}_k, \bar{\mathbf{A}}_{k-1}; \bar{\mathbf{C}}_{k-1} = \mathbf{0})$ as $g_{A,k}$ and $g_{C,k}(\bar{\mathbf{L}}_k, \bar{\mathbf{A}}_k; \bar{\mathbf{C}}_{k-1} = \mathbf{0})$ as $g_{C,k}$. Define $g_{A,C} = \prod_{k=0}^K g_{A,k} g_{C,k}$ and let $\hat{g}_{A,C} = \prod_{k=0}^K \hat{g}_{A,k} \hat{g}_{C,k}$ be an estimator of $g_{A,C}$ using a model for treatment assignment and a model for being censored at each time. Last, let $\hat{g}_{A,C,i}$ be a prediction from the model $\hat{g}_{A,C}$ for the i th individual (i.e., the predicted probability that the i th individual follows the treatment regime \mathbf{a} and is not censored). Using the sample analog of

identification result in equation (3), the IPW estimator is given by

$$\hat{\mu}_{\text{IPW}}(w) = \frac{\sum_{\mathbf{L}_{0,i} \in w} \frac{I(\mathbf{A}_i=\mathbf{a}, \mathbf{C}_i=\mathbf{0})Y_{K+1,i}}{\hat{g}_{A,C,i}}}{\sum_{\mathbf{L}_{0,i} \in w} \frac{I(\mathbf{A}_i=\mathbf{a}, \mathbf{C}_i=\mathbf{0})}{\hat{g}_{A,C,i}}}.$$

If $\hat{g}_{A,C}$ consistently estimates $g_{A,C}$, the IPW estimator is consistent.

The g-computation estimator, sometimes referred to as the iterative conditional expectation estimator [Wen et al., 2021], is calculated by iteratively estimating the conditional expectations in identification result (4), where all the estimators for the conditional expectation are restricted to data from subgroup w . That is, the g-computation estimator is implemented using the following steps:

1. Estimate $E[Y_{K+1}|\mathbf{A}, \mathbf{L}]$ using data from individuals that did not dropout (i.e., $\mathbf{C} = \mathbf{0}$). Use the estimator to create predictions for each individual with $\bar{\mathbf{C}}_{K-1} = \mathbf{0}$ setting their treatment regime to $\mathbf{A} = \mathbf{a}$. Denote the predictions by \hat{Q}_{K+1} .
2. Use \hat{Q}_{K+1} as a pseudo-outcome and estimate the conditional expectation of \hat{Q}_{K+1} conditional on $\bar{\mathbf{A}}_{K-1}$ and $\bar{\mathbf{L}}_{K-1}$ among those with $\bar{\mathbf{C}}_{K-1} = \mathbf{0}$. Use the estimator to create predictions \hat{Q}_K . Repeat this iterative process until the conditional expectation that is estimated is only conditional on treatment at the baseline visit A_0 and the baseline covariates \mathbf{L}_0 . Denote the resulting predictions by \hat{Q}_1 .
3. The g-computation estimator is calculated as the subgroup average of the predictions \hat{Q}_1 .

The g-computation estimator is consistent if all the conditional expectation estimators required for its implementation are consistent.

The longitudinal TMLE is similar to the g-computation estimator described above, but it updates the conditional expectation of the outcome in each iterative conditional expectation model above using the treatment regime and dropout information, targeted to reduce bias [Kreif et al., 2017, van der Laan and Gruber, 2012]. Specifically, in the first step of obtaining the g-computation estimator, we use an additional “targeting” step where we fit an intercept only model using Y_{K+1} as the outcome with \hat{Q}_{K+1} as an offset and with weights $\frac{I(\mathbf{A}=\mathbf{a}, \mathbf{C}=\mathbf{0})}{\hat{g}_{A,C}}$. We denote the resulting predic-

tions by \widehat{Q}_{K+1}^* and this targeting step is performed for each iterative conditional expectation. The TMLE estimator is then calculated as the subgroup average of the predictions \widehat{Q}_1^* . In contrast to the inverse probability weighting and g-computation estimators, TMLE is doubly robust [van der Laan and Gruber, 2012]. That is, it is consistent for the potential outcome mean when either i) all models for the treatment assignment and the dropout probability are correctly specified or ii) all models for the conditional expectation of the outcome are correctly specified. It is semi-parametric efficient when all the models are correctly specified [van der Laan and Gruber, 2012]. TMLE is a substitution estimator, and is therefore, under mild assumptions, guaranteed to fall within the support of the outcome Y_{K+1} . While we focus on TMLE in the remainder of the manuscript, the IPW, g-computation or other estimators such as the doubly robust estimator [Bang and Robins, 2005] could be used.

3.3 Subgroup Discovery for Longitudinal Data (SDLD) algorithm

The Subgroup Discovery for Longitudinal Data (SDLD) algorithm is defined by using the longitudinal TMLE as the treatment effect estimator in the generalized interaction tree algorithm. In Appendix C we present simulations that show good finite sample performance of the SDLD algorithm for identifying the correct subgroups. The SDLD algorithm splits the covariate space into disjoint and exhaustive subgroups based on maximizing between subgroup treatment effect heterogeneity and within each subgroup a treatment effect estimator is calculated (terminal node estimator). The following theorem is proved in Appendix B.

Theorem 1. *If Assumptions B.1-B.5 in Appendix B hold, the SDLD algorithm is L_2 consistent.*

At each splitting decision, the SDLD algorithm discovers subgroups by searching over all possible covariate and split-point combinations and selecting the combination that maximizes between subgroup heterogeneity estimated by the splitting criterion (1). As a result, the observed treatment effect heterogeneity is likely overestimated and that results in bias in the subgroup-specific treatment effect estimators. Data splitting can be used to get unbiased subgroup-specific treatment effect estimators [Fithian et al., 2014, Yang et al., 2022]. Data splitting separates the data into two disjoint and exhaustive parts. One part is used for fitting the SDLD algorithm and producing a

list of subgroups and the other part is used for subgroup-specific treatment effect estimation and confidence interval construction. As the data used for subgroup discovery and subgroup-specific treatment effect estimation are independent, the data splitting process results in unbiased treatment effect estimators and asymptotically valid confidence intervals.

4 Discovering subgroups with differential weight gain when on DTG-containing ARTs versus non DTG-containing ARTs

DTG is an antiretroviral medication that belongs to the class of integrase strand transfer inhibitors. In combination with other medications, DTG has shown promising results in clinical trials and is globally used today [Kandel and Walmsley, 2015]. A concern with DTG-containing antiretroviral therapies (ARTs) has been the emergence of substantial weight gain as a potential side effect. A recent phase III trial conducted in South Africa [Venter et al., 2019, 2020] compared two DTG-containing ARTs to standard of care over a 96-week follow-up period. Substantially higher weight gains were seen in the two groups receiving DTG-containing ARTs compared to the standard of care group. Another phase III trial conducted in Cameroon also showed larger weight gains when on DTG-containing ART compared to a low-dose efavirenz-based ART [NAMSAL ANRS 12313 Study Group, 2019, Calmy et al., 2020]. Of particular concern is that Lake [2017] found that weight gain associated with DTG-containing ARTs has been shown to be associated with increased truncal fat, a known risk factor for adverse cardiovascular outcomes among people living with HIV.

Not all people are expected to be at the same risk for increased weight gain associated with DTG-containing ARTs. In the South African trial previously described, weight gain was greater for females and people with lower CD4 counts or higher viral loads. Similarly, in the Cameroon trial weight gain was more severe among women. Discovering subgroups of people for whom being on DTG-containing ARTs is more likely to cause substantial weight gain can help the development of treatment recommendations or monitoring plans tailored to a person's risk profile.

The Academic Model Providing Access to Healthcare (AMPATH) partnership is a consortium of research institutions focusing on prevention and treatment of HIV in western Kenya [Tierney

et al., 2007]. AMPATH administers the AMPATH’s open-source electronic medical record system (AMRS), which is a large-scale electronic health record database that has information on clinical encounters, lab measurements, and demographic characteristics. We implemented the SDDL algorithm on data from AMRS to discover subgroups with differential effect of DTG-containing ARTs on weight.

We included people living with HIV who were at least 18 years old, were initiating or on ART, and had data on or after July 1, 2016 in AMRS. A total of 88,367 people living with HIV met these inclusion criteria. For each individual, we defined time 0 as July 1, 2016 if the person was enrolled in AMPATH before that time and as the enrollment date at AMPATH if the person was enrolled after July 1, 2016. To structure the data, we used time periods with a length of 200 days and captured data at time k within days $[200k, 200(k + 1))$, for $k \in \{0, \dots, K + 1\}$ (e.g., we used data from days 0-199 to create L_0, A_0, C_0 and days 200-399 to create L_1, A_1, C_1). We focused on the first five time periods (1,000 days) as the data on people that were always on DTG-containing ARTs became sparse over time, resulting in unstable estimates over longer follow-up. We censored individuals at time k if there was no clinical visit in the time periods after time k . As pregnancy leads to natural weight gain, we excluded 1,475 women that were pregnant at baseline and censored individuals at time $k - 1$ if they were first recorded as pregnant at time k , $k = 1, \dots, K$. Last, we excluded one individual who had an data entry error whose ART start date was recorded before date of birth and 2,446 individuals that had no outcome or treatment information available in any time period. Hence, the analysis set consisted of 84,445 individuals who had a total of 1,178,016 unique clinical visits.

The outcome of interest was weight in kilograms at time 4 (i.e., Y_4 collected within days 800-999). Treatment at each time was defined as 1 if an individual was receiving a DTG-containing ART, and 0 if not. The two treatment regimes of interest were always on and never on DTG-containing ART. We included HIV viral load, systolic blood pressure, diastolic blood pressure, weight, height, whether the individual had active tuberculosis, was being treated for tuberculosis, was married or living with partner, and whether the individual was covered by the National Health Insurance Fund as time-dependent covariates. The vector of baseline covariates L_0 included the

values of time-varying covariates at time 0, gender, age when starting ART, age at time 0, time on ART at time 0, and whether the individual was enrolled on or after July 1, 2016. Further details on how we pre-processed the data and how we handled missing data and multiple clinic visits within each time period are provided in Appendix D.

When implementing the SDL algorithm, we applied data splitting by randomly selecting 60% of the dataset (50,666 individuals) for tree building using the SDL algorithm and 40% (33,779 individuals) for subgroup-specific treatment effect estimation. In the tree building dataset, we randomly sampled 80% (40,533 individuals) for initial tree building and used the remaining 20% (10,133 individuals) as the validation set used for final tree selection. In the treatment effect estimation dataset, we constructed confidence intervals for treatment effects using the non-parametric bootstrap with 1,000 bootstrap samples.

Implementing the SDL algorithm requires estimating models for the probability of treatment assignment, the probability of dropping out of the study, and the estimation of the pseudo-outcome at each time. For all these models, we used generalized linear regression models with linear and additive main effects for all past covariate and treatment variables.

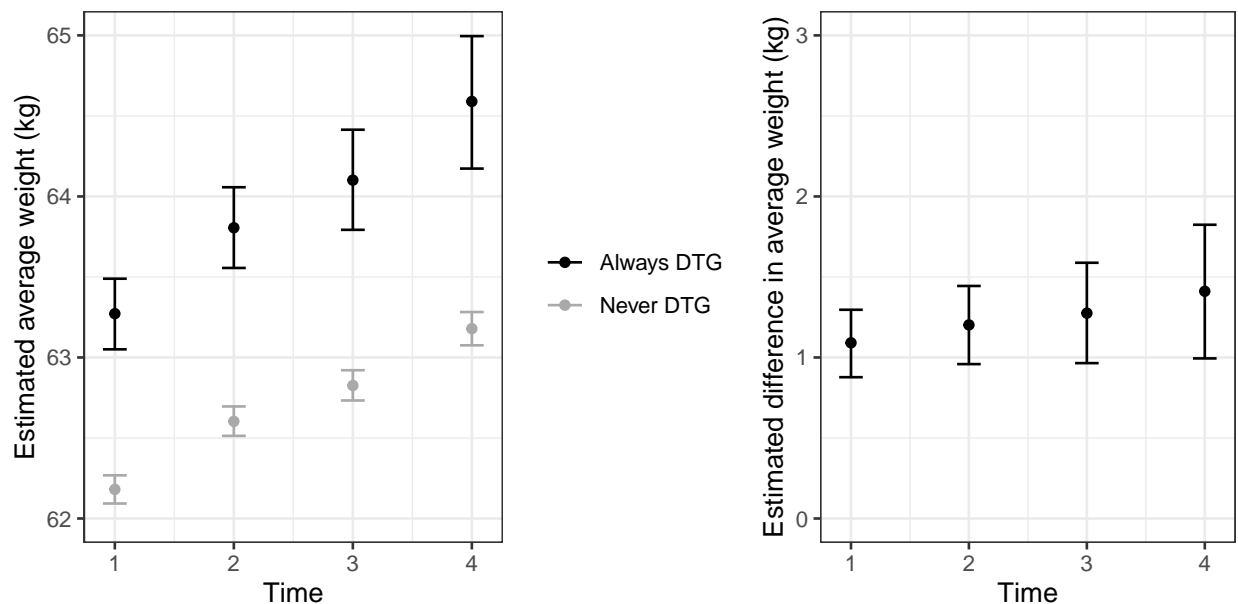


Figure 1: Estimated average weight (left) using targeted maximum likelihood estimation (TMLE) if always and never being on a DTG-containing ART and estimated causal effect on average weight (right) comparing always versus never being on a DTG-containing ART at each time. Error bars show 95% confidence intervals estimated using the non-parametric bootstrap.

Figure 1 shows the estimated average weight had all individuals been always or never on DTG-containing ARTs (left) and the average weight gain when comparing always being on DTG-containing ARTs to never being on DTG-containing ARTs (right) at each time. The confidence intervals are estimated using the non-parametric bootstrap with 10,000 bootstrap samples. The numerical values of the estimates and the corresponding confidence intervals used for making Figure 1 are included in Appendix D. The results show that sustained treatment with a DTG-containing ART leads to increased weight gain compared to never receiving DTG; the estimated weight gain increases from 1.09 kilograms at time one (i.e., days 200-399) to 1.41 kilograms at time four (i.e., days 800-999).

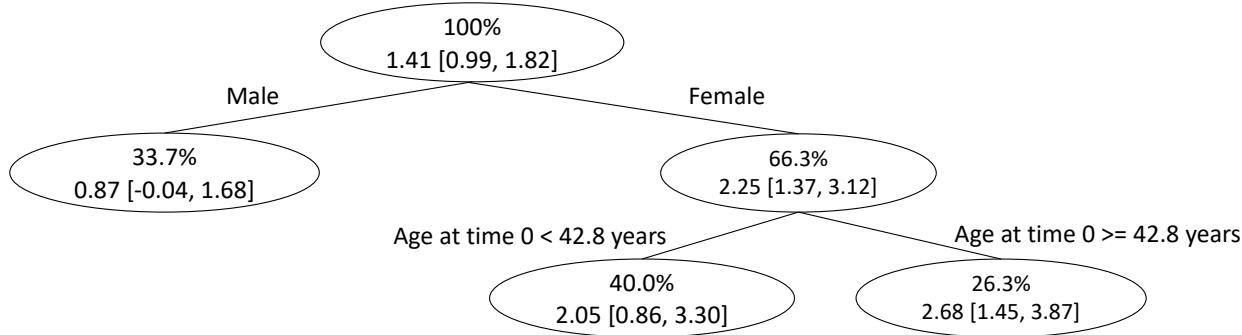


Figure 2: Final tree structure when the SDDL algorithm is applied to data from electronic health records on people living with HIV in western Kenya to discover subgroups with heterogeneous effects of DTG-containing ARTs on weight gain. Within each subgroup, the first row shows the percentage of the dataset that belongs to the subgroup and the second row shows the estimated weight gain comparing being always versus never on DTG-containing ARTs and associated 95% confidence interval.

Figure 2 shows the final tree structure produced by the SDDL algorithm with subgroup-specific treatment effect estimates and associated 95% confidence intervals. The final tree first splits on gender and then makes another split depending on whether the females are younger or older than 42.8 years old at baseline. The results suggest that the effects of DTG-containing ARTs are larger for females than males (2.25 vs 0.87 kg) although the 95% bootstrap confidence intervals are slightly overlapping ($[-0.04, 1.68]$ for males and $[1.37, 3.12]$ for females). Results from randomized trials and other data-sources support the finding that additional weight gains due to being on DTG-containing ARTs are larger among females than males [Bourgi et al., 2020a, Calmy et al., 2020, Sax et al.,

2020, Venter et al., 2020]. The effect of DTG-containing ARTs is estimated to be 2.05 kilograms among females that are younger than 42.8 years old and 2.68 kilograms among females that are older than or equal to 42.8 years old, but the corresponding bootstrap confidence intervals are highly overlapping ($[0.86, 3.30]$ for younger females and $[1.45, 3.87]$ for older females). In Appendix D we present details on the estimated average weight gain from receiving DTG-containing ARTs at each time in the subgroups discovered by the SDDL algorithm and the stability of the trees produced by the SDDL algorithm.

5 Discussion

We developed the Subgroup Discovery for Longitudinal Data (SDDL) algorithm for discovering subgroups with heterogeneous treatment effects using longitudinal observational data. The algorithm combines the generalized interaction tree algorithm with longitudinal targeted maximum likelihood estimation and can handle time-varying non-randomized treatment assignment and dropout. We used the algorithm to discover subgroups of individuals with differential weight gain when receiving DTG-containing ARTs using data from AMPATH. Our results suggest that gender is the primary modifier of weight gain from receiving DTG-containing ARTs versus non DTG-containing ARTs, with females gaining more weight than males. This result is consistent with prior literature where subgroup analyses using pre-specified subgroups (not data-driven subgroup discovery) showed larger weight gains among females.

Our analysis focused on comparing DTG-containing ARTs to other non DTG-containing ARTs and did not distinguish among different antiretroviral medications included in DTG-containing ARTs. Previous studies have evaluated different DTG-containing ARTs [Venter et al., 2019] and the results show that the weight gains might differ depending on what medications DTG is combined with. Further investigation into specific DTG-containing ARTs might provide a more fine-grained understanding of the effect of DTG on weight gain.

The SDDL algorithm defines subgroups based on baseline covariates. Extending the algorithm to dynamically update the subgroups when new information becomes available is of interest [Sun et al., 2020]. Although our application focuses on always and never receiving DTG-containing

ARTs, the SDLD algorithm can accommodate other treatment regimes as well. Furthermore, the SDLD algorithm results in a single tree structure that creates an interpretable treatment effect stratification rule by partitioning the covariate space into identifiable subgroups with differential treatment effects. Ensemble methods, such as random forest or bagging, average multiple single trees with the aim of improving prediction accuracy. However, the resulting black-box model no longer has the structure of a single tree and unlike the single tree it does not discover clinically interpretable subgroups. It would be of interest to develop ensemble based methods for prediction with EHR data using trees built by the SDLD algorithm as the building block.

Acknowledgements

This work was supported in part by Patient-Centered Outcomes Research Institute (PCORI) awards ME-2019C3-17875, ME-2021C2-22365; National Library of Medicine (NLM) grant R01LM013616 and National Institute of Allergy and Infectious Diseases (NIAID) awards P30AI042853, R01AI167694 and K24AI134359. The content is solely the responsibility of the authors and does not necessarily represent the official views of the NLM, NIAID, PCORI, PCORI's Board of Governors, or PCORI's Methodology Committee.

References

- A. Achhra, A. Mocroft, P. Reiss, C. Sabin, L. Ryom, S. De Wit, C. Smith, A. d'Arminio Monforte, A. Phillips, R. Weber, et al. Short-term weight gain after antiretroviral therapy initiation and subsequent risk of cardiovascular disease and diabetes: the d: A: D study. *HIV medicine*, 17(4): 255–268, 2016.
- S. Athey and G. Imbens. Recursive partitioning for heterogeneous causal effects. *Proceedings of the National Academy of Sciences*, 113(27):7353–7360, 2016.
- H. Bang and J. M. Robins. Doubly robust estimation in missing data and causal inference models. *Biometrics*, 61(4):962–973, 2005.
- K. Bourgi, C. A. Jenkins, P. F. Rebeiro, B. E. Shepherd, F. Palella, R. D. Moore, K. N. Althoff, J. Gill, C. S. Rabkin, S. J. Gange, et al. Weight gain among treatment-naïve persons with hiv starting integrase inhibitors compared to non-nucleoside reverse transcriptase inhibitors or protease inhibitors in a large observational cohort in the united states and canada. *Journal of the International AIDS Society*, 23(4):e25484, 2020a.
- K. Bourgi, P. F. Rebeiro, M. Turner, J. L. Castilho, T. Hulgan, S. P. Raffanti, J. R. Koethe, and T. R. Sterling. Greater weight gain in treatment-naive persons starting dolutegravir-based antiretroviral therapy. *Clinical Infectious Diseases*, 70(7):1267–1274, 2020b.
- L. Breiman, J. Friedman, R. Olshen, and C. Stone. Classification and regression trees. wadsworth int. Group, 37(15):237–251, 1984.
- A. Calmy, T. T. Sanchez, C. Kouanfack, M. Mpoudi-Etame, S. Leroy, S. Perrineau, M. L. Wandji, D. T. Tata, P. O. Bassega, T. A. Bwenda, et al. Dolutegravir-based and low-dose efavirenz-based regimen for the initial treatment of hiv-1 infection (namsal): week 96 results from a two-group, multicentre, randomised, open label, phase 3 non-inferiority trial in cameroon. *The lancet HIV*, 7(10):e677–e687, 2020.
- I. J. Dahabreh, R. Hayward, and D. M. Kent. Using group data to treat individuals: understanding

- heterogeneous treatment effects in the age of precision medicine and patient-centred evidence. *International journal of epidemiology*, 45(6):2184–2193, 2016.
- A. L. Esber, D. Chang, M. Iroezindu, E. Bahemana, H. Kibuuka, J. Owuoth, V. Singoei, J. Maswai, N. F. Dear, T. A. Crowell, et al. Weight gain during the dolutegravir transition in the african cohort study. *Journal of the International AIDS Society*, 25(4):e25899, 2022.
- W. Fithian, D. Sun, and J. Taylor. Optimal inference after model selection. *arXiv preprint arXiv:1410.2597*, 2014.
- J. C. Foster, J. M. Taylor, and S. J. Ruberg. Subgroup identification from randomized clinical trial data. *Statistics in medicine*, 30(24):2867–2880, 2011.
- M. Herrin, J. P. Tate, K. M. Akgün, A. A. Butt, K. Crothers, M. S. Freiberg, C. L. Gibert, D. A. Leaf, D. Rimland, M. C. Rodriguez-Barradas, et al. Weight gain and incident diabetes among hiv infected-veterans initiating antiretroviral therapy compared to uninfected individuals. *Journal of acquired immune deficiency syndromes (1999)*, 73(2):228, 2016.
- C. E. Kandel and S. L. Walmsley. Dolutegravir—a review of the pharmacology, efficacy, and safety in the treatment of hiv. *Drug design, development and therapy*, 9:3547, 2015.
- D. J. Kim, A. O. Westfall, E. Chamot, A. L. Willig, M. J. Mugavero, C. Ritchie, G. A. Burkholder, H. M. Crane, J. L. Raper, M. S. Saag, et al. Multimorbidity patterns in hiv-infected patients: the role of obesity in chronic disease clustering. *Journal of acquired immune deficiency syndromes (1999)*, 61(5):600, 2012.
- N. Kreif, L. Tran, R. Grieve, B. De Stavola, R. C. Tasker, and M. Petersen. Estimating the comparative effectiveness of feeding interventions in the pediatric intensive care unit: a demonstration of longitudinal targeted maximum likelihood estimation. *American journal of epidemiology*, 186(12):1370–1379, 2017.
- J. E. Lake. The fat of the matter: obesity and visceral adiposity in treated hiv infection. *Current HIV/AIDS Reports*, 14(6):211–219, 2017.

- NAMSAL ANRS 12313 Study Group. Dolutegravir-based or low-dose efavirenz-based regimen for the treatment of hiv-1. *New England Journal of Medicine*, 381(9):816–826, 2019.
- A. Nobel. Histogram regression estimation using data-dependent partitions. *The Annals of Statistics*, 24(3):1084–1105, 1996.
- J. Pearl and J. M. Robins. Probabilistic evaluation of sequential plans from causal models with hidden variables. In *UAI*, volume 95, pages 444–453. Citeseer, 1995.
- M. Petersen, J. Schwab, S. Gruber, N. Blaser, M. Schomaker, and M. van der Laan. Targeted maximum likelihood estimation for dynamic and static longitudinal marginal structural working models. *Journal of causal inference*, 2(2):147–185, 2014.
- A. N. Phillips, F. Venter, D. Havlir, A. Pozniak, D. Kuritzkes, A. Wensing, J. D. Lundgren, A. De Luca, D. Pillay, J. Mellors, et al. Risks and benefits of dolutegravir-based antiretroviral drug regimens in sub-saharan africa: a modelling study. *The Lancet HIV*, 6(2):e116–e127, 2019.
- J. Robins. A new approach to causal inference in mortality studies with a sustained exposure period—application to control of the healthy worker survivor effect. *Mathematical modelling*, 7(9-12):1393–1512, 1986.
- J. M. Robins and S. Greenland. Causal inference without counterfactuals: comment. *Journal of the American Statistical Association*, 95(450):431–435, 2000.
- J. M. Robins and A. Rotnitzky. Recovery of information and adjustment for dependent censoring using surrogate markers. In *AIDS epidemiology*, pages 297–331. Springer, 1992.
- J. M. Robins, A. Rotnitzky, and L. P. Zhao. Estimation of regression coefficients when some regressors are not always observed. *Journal of the American statistical Association*, 89(427):846–866, 1994.
- D. B. Rubin. Estimating causal effects of treatments in randomized and nonrandomized studies. *Journal of educational Psychology*, 66(5):688, 1974.

- P. E. Sax, K. M. Erlandson, J. E. Lake, G. A. Mccomsey, C. Orkin, S. Esser, T. T. Brown, J. K. Rockstroh, X. Wei, C. C. Carter, et al. Weight gain following initiation of antiretroviral therapy: risk factors in randomized comparative clinical trials. *Clinical Infectious Diseases*, 71(6):1379–1389, 2020.
- H. Seibold, A. Zeileis, and T. Hothorn. Model-based recursive partitioning for subgroup analyses. *The international journal of biostatistics*, 12(1):45–63, 2016.
- J. A. Steingrimsson and J. Yang. Subgroup identification using covariate-adjusted interaction trees. *Statistics in medicine*, 2019.
- J. A. Steingrimsson, L. Diao, A. M. Molinaro, and R. L. Strawderman. Doubly robust survival trees. *Statistics in medicine*, 35(20):3595–3612, 2016.
- O. M. Stitelman, V. De Gruttola, and M. J. van der Laan. A general implementation of tmlc for longitudinal data applied to causal inference in survival analysis. *The international journal of biostatistics*, 8(1), 2012.
- X. Su, T. Zhou, X. Yan, J. Fan, and S. Yang. Interaction trees with censored survival data. *The international journal of biostatistics*, 4(1), 2008.
- X. Su, C.-L. Tsai, H. Wang, D. M. Nickerson, and B. Li. Subgroup analysis via recursive partitioning. *Journal of Machine Learning Research*, 10(Feb):141–158, 2009.
- X. Su, K. Meneses, P. McNees, and W. O. Johnson. Interaction trees: exploring the differential effects of an intervention programme for breast cancer survivors. *Journal of the Royal Statistical Society: Series C (Applied Statistics)*, 60(3):457–474, 2011.
- Y. Sun, S. H. Chiou, C. O. Wu, M. McGarry, and C.-Y. Huang. Dynamic risk prediction using survival tree ensembles with application to cystic fibrosis. *arXiv preprint arXiv:2011.07175*, 2020.
- B. Surial, C. Mugglin, A. Calmy, M. Cavassini, H. F. Günthard, M. Stöckle, E. Bernasconi, P. Schmid, P. E. Tarr, H. Furrer, et al. Weight and metabolic changes after switching from

- tenofovir disoproxil fumarate to tenofovir alafenamide in people living with hiv: a cohort study. *Annals of internal medicine*, 174(6):758–767, 2021.
- W. M. Tierney, J. K. Rotich, T. J. Hannan, A. M. Siika, P. G. Biondich, B. W. Mamlin, W. M. Nyandiko, S. Kimaiyo, K. Wools-Kaloustian, J. E. Sidle, et al. The ampath medical record system: creating, implementing, and sustaining an electronic medical record system to support hiv/aids care in western kenya. *Studies in health technology and informatics*, 129(1):372, 2007.
- M. J. van der Laan and S. Gruber. Targeted minimum loss based estimation of causal effects of multiple time point interventions. *The international journal of biostatistics*, 8(1), 2012.
- M. J. Van der Laan and S. Rose. *Targeted learning in data science*. Springer, 2018.
- M. J. Van Der Laan and D. Rubin. Targeted maximum likelihood learning. *The international journal of biostatistics*, 2(1), 2006.
- M. J. Van der Laan, S. Rose, et al. *Targeted learning: causal inference for observational and experimental data*, volume 4. Springer, 2011.
- W. D. Venter, M. Moorhouse, S. Sokhela, L. Fairlie, N. Mashabane, M. Masenya, C. Serenata, G. Akpomiemie, A. Qavi, N. Chandiwana, et al. Dolutegravir plus two different prodrugs of tenofovir to treat hiv. *New England Journal of Medicine*, 381(9):803–815, 2019.
- W. D. Venter, S. Sokhela, B. Simmons, M. Moorhouse, L. Fairlie, N. Mashabane, C. Serenata, G. Akpomiemie, M. Masenya, A. Qavi, et al. Dolutegravir with emtricitabine and tenofovir alafenamide or tenofovir disoproxil fumarate versus efavirenz, emtricitabine, and tenofovir disoproxil fumarate for initial treatment of hiv-1 infection (advance): week 96 results from a randomised, phase 3, non-inferiority trial. *The Lancet HIV*, 7(10):e666–e676, 2020.
- Y. Wei, L. Liu, X. Su, L. Zhao, and H. Jiang. Precision medicine: Subgroup identification in longitudinal trajectories. *Statistical methods in medical research*, 29(9):2603–2616, 2020.
- L. Wen, J. G. Young, J. M. Robins, and M. A. Hernán. Parametric g-formula implementations for causal survival analyses. *Biometrics*, 77(2):740–753, 2021.

World Health Organization. *Consolidated guidelines on the use of antiretroviral drugs for treating and preventing HIV infection: recommendations for a public health approach*. World Health Organization, 2016.

World Health Organization. Updated recommendations on first-line and second-line antiretroviral regimens and post-exposure prophylaxis and recommendations on early infant diagnosis of hiv: interim guidelines: supplement to the 2016 consolidated guidelines on the use of antiretroviral drugs for treating and preventing hiv infection. Technical report, World Health Organization, 2018.

J. Yang, I. J. Dahabreh, and J. A. Steingrimsson. Causal interaction trees: Finding subgroups with heterogeneous treatment effects in observational data. *Biometrics*, 78(2):624–635, 2022.

Appendix A Pruning step of SDLD algorithm

In this section we describe the the pruning step of the SDLD algorithm. The initial tree building step results in a large tree that usually substantially overfits the data. The goal of the pruning step is to create a sequence of subtrees of the initial tree that are candidates for being the final tree (model). This substantially reduces the computational complexity compared to looking at all possible subtrees.

The pruning algorithm we use is an extension of weakest link pruning [Breiman et al., 1984] to the setting of causal treatment effect estimation [Su et al., 2008]. The algorithm builds a sequence of subtrees of $\widehat{\psi}_{\max}$ by sequentially cutting the “weakest link” defined as the branch of the tree with the smallest split complexity.

For a non-terminal node h define the branch that consists of the node h and all its descendants as ψ_h^* . The split complexity of the subtree ψ_h^* is zero at

$$\lambda^* = \frac{\sum_{w \in W_{\psi_h^*}} G_w(\psi_h^*)}{|W_{\psi_h^*}|}.$$

If the objective is to maximize split complexity, removing the branch ψ_h^* is preferred if $\lambda > \lambda^*$, and keeping branch ψ_h^* is preferred if $\lambda < \lambda^*$. Weakest link pruning is given by the following steps:

1. Initialize the algorithm by setting $\widehat{\psi}_0 = \widehat{\psi}_{\max}$ and set $d = 0$.

2. Set $d = d + 1$.

3. Define a function

$$g(h) = \begin{cases} \frac{\sum_{w \in W_{\psi_h^*}} G_w(\psi_h^*)}{|W_{\psi_h^*}|} & \text{if } h \in W_{\widehat{\psi}_{d-1}} \\ \infty & \text{otherwise.} \end{cases}$$

The weakest branch of the tree is the branch rooted in node $h = \arg \min_{h' \in W_{\widehat{\psi}_{d-1}}} g(h')$. Define the subtree $\widehat{\psi}_d$ as the subtree of $\widehat{\psi}_{d-1}$ with all descendants of node h removed.

4. Repeat steps 2 and 3 until the tree $\widehat{\psi}_d$ consists only of the root node.

The weakest link pruning algorithm creates a finite sequence of trees $\widehat{\psi}_0, \dots, \widehat{\psi}_{\widehat{D}}$. The final tree

selection step selects a single tree from this algorithm.

Appendix B Consistency of SDLD algorithm

In this section we show that the Subgroup Discovery for Longitudinal Data (SDLD) algorithm is L_2 consistent. Recall that \mathcal{L}_0 is the sample space of \mathbf{L}_0 and further let \mathcal{L}_k be the sample space of \mathbf{L}_k , $k \in \{1, \dots, K\}$; assume that the outcome of interest at visit $K + 1$ is bounded, $|Y_{K+1}| \leq B_1 < \infty$; define the sample space of the observed data as $\mathcal{O} = \mathcal{L}_0 \times \{0, 1\} \times \{0, 1\} \times \mathcal{L}_1 \times \dots \times [-B_1, B_1]$. Borrowing notation from Nobel [1996], let π be any partition of \mathcal{L}_0 and define Π as the range of π ; let $\hat{\psi}_n$ be an empirical rule (tree) with \widehat{M}_n partitions (nodes) and define Π_n as the range of $\hat{\psi}_n$. For each element $\pi = \{u_k\} \in \Pi$, define an associated partition $\tilde{\pi} = \{u_k \times \{0, 1\} \times \dots \times [-B_1, B_1]\}$ on \mathcal{O} and let $\tilde{\Pi}$ be the range of $\tilde{\pi}$. Analogously, for each element $\pi_n = \{w_k\} \in \Pi_n$, define an associated partition $\tilde{\pi}_n = \{w_k \times \{0, 1\} \times \dots \times [-B_1, B_1]\}$ on \mathcal{O} and let $\tilde{\Pi}_n$ be the range of $\tilde{\pi}_n$. Finally, let $w_\pi(\mathbf{l}_0)$ be the unique partition (terminal node) in partition rule π that contains the covariate vector \mathbf{l}_0 .

Define $\boldsymbol{\theta}_{w_\pi(\mathbf{l}_0)}^{\mathbf{a}}$ as a vector of the nuisance parameters used to implement TMLE for treatment regime \mathbf{a} estimated using data from the terminal node $w_\pi(\mathbf{l}_0)$. These nuisance parameters include those used to index the models for the probability of treatment assignment, probability of being censored, and the model for the conditional expectation of the outcome. The TMLE for $E[Y_{K+1}^{\mathbf{a}, c=0} | \mathbf{L}_0 \in w_\pi(\mathbf{l}_0)]$ is given by averaging over the predictions from all observations that condition on $\mathbf{L}_0 \in w_\pi(\mathbf{l}_0)$. Let $Y_{i, w_\pi(\mathbf{l}_0)}^{*, \mathbf{a}} \{\mathbf{O}; \boldsymbol{\theta}_{w_\pi(\mathbf{l}_0)}^{\mathbf{a}}\}$ be the prediction from the i th individual used to calculate that average. Define the transformed outcome

$$Y_{i, w_\pi(\mathbf{l}_0)}^* \{\mathbf{O}; \boldsymbol{\theta}_{w_\pi(\mathbf{l}_0)}\} = Y_{i, w_\pi(\mathbf{l}_0)}^{*, \mathbf{a}_1} \{\mathbf{O}; \boldsymbol{\theta}_{w_\pi(\mathbf{l}_0)}^{\mathbf{a}_1}\} - Y_{i, w_\pi(\mathbf{l}_0)}^{*, \mathbf{a}_0} \{\mathbf{O}; \boldsymbol{\theta}_{w_\pi(\mathbf{l}_0)}^{\mathbf{a}_0}\},$$

where $\boldsymbol{\theta}_{w_\pi(\mathbf{l}_0)} = (\boldsymbol{\theta}_{w_\pi(\mathbf{l}_0)}^{\mathbf{a}_0}, \boldsymbol{\theta}_{w_\pi(\mathbf{l}_0)}^{\mathbf{a}_1})$. For simplicity of notation, we denote the transformed outcome as $Y_{i, w_\pi(\mathbf{l}_0)}^* (\boldsymbol{\theta}_{w_\pi(\mathbf{l}_0)})$.

Define $r(\mathbf{l}_0) = E[Y_{K+1}^{\mathbf{a}_1, c=0} | \mathbf{L}_0 = \mathbf{l}_0] - E[Y_{K+1}^{\mathbf{a}_0, c=0} | \mathbf{L}_0 = \mathbf{l}_0]$ and the tree estimator for $r(\mathbf{l}_0)$ is given

by

$$\hat{r}_n(\mathbf{l}_0) = \frac{\sum_{i=1}^n I\{\mathbf{L}_{0,i} \in w_{\hat{\psi}_n}(\mathbf{l}_0)\} Y_{i,w_{\hat{\psi}_n}(\mathbf{l}_0)}^* \left(\hat{\boldsymbol{\theta}}_{w_{\hat{\psi}_n}(\mathbf{l}_0)} \right)}{\sum_{i=1}^n I\{\mathbf{L}_{0,i} \in w_{\hat{\psi}_n}(\mathbf{l}_0)\}}.$$

The following theorem shows that the SDDL algorithm is L_2 consistent.

Theorem 2. *Assume that*

B.1 Y_{K+1} is bounded such that $|Y_{K+1}| \leq B_1 < \infty$.

B.2 The number of terminal nodes $\widehat{M}_n \rightarrow \infty$ and $\widehat{M}_n = o\left\{\frac{n}{\log(n)}\right\}$.

B.3 The derivative $\frac{\partial Y_{w_{\pi_n}(\mathbf{l}_0)}^(\boldsymbol{\theta}_{w_{\pi_n}(\mathbf{l}_0)})}{\partial \boldsymbol{\theta}_{w_{\pi_n}(\mathbf{l}_0)}} \Big|_{\boldsymbol{\theta}_{w_{\pi_n}(\mathbf{l}_0)} = \boldsymbol{\theta}_{w_{\pi_n}(\mathbf{l}_0)}^*}$ exists for $\pi_n \in \Pi_n$ and is uniformly bounded, where $\boldsymbol{\theta}_{w_{\pi_n}(\mathbf{l}_0)}^*$ is the asymptotic almost sure limit of $\hat{\boldsymbol{\theta}}_{w_{\pi_n}(\mathbf{l}_0)}$.*

B.4 For given \mathbf{a} and \mathbf{c} , any $\tilde{\pi} = \{\tilde{u}_k\} \in \tilde{\Pi}$ and $\mathbf{o} \in \tilde{u}_k$, either the iterated conditional expectation of the observed outcome or the treatment regime mechanism and the censoring mechanism are correctly specified (necessary condition for consistency of TMLE).

B.5 The models \hat{g}_A and \hat{g}_C are uniformly bounded away from zero.

If conditions B.1 through B.5 hold, the Subgroup Discovery for Longitudinal Data (SDDL) algorithm is L_2 consistent.

Proof of Theorem 2: Define

$$\tilde{r}_n(\mathbf{l}_0) = \frac{\sum_{i=1}^n I\{\mathbf{L}_{0,i} \in w_{\hat{\psi}_n}(\mathbf{l}_0)\} r(\mathbf{L}_{0,i})}{\sum_{i=1}^n I\{\mathbf{L}_{0,i} \in w_{\hat{\psi}_n}(\mathbf{l}_0)\}}.$$

We can show that

$$\int_{\mathcal{L}_0} |r(\mathbf{l}_0) - \hat{r}_n(\mathbf{l}_0)|^2 d\mathbf{P}(\mathbf{l}_0) \leq 2 \int_{\mathcal{L}_0} |\hat{r}_n(\mathbf{l}_0) - \tilde{r}_n(\mathbf{l}_0)|^2 d\mathbf{P}(\mathbf{l}_0) + 2 \int_{\mathcal{L}_0} |r(\mathbf{l}_0) - \tilde{r}_n(\mathbf{l}_0)|^2 d\mathbf{P}(\mathbf{l}_0),$$

where $\mathbf{P}(\mathbf{l}_0)$ is the distribution function for \mathbf{l}_0 . We will show that both terms on the right hand side of the above equation are $o_P(1)$ which shows that $\hat{r}_n(\mathbf{l}_0)$ is L_2 consistent.

Assumptions B.1 and B.5 ensure that there exists a $B_2 > 0$ such that

$$\max \left\{ \left| Y_{w\pi_n}^* \left(\widehat{\boldsymbol{\theta}}_{w\pi_n}(\mathbf{l}_0) \right) \right|, \left| Y_{w\pi_n}^* \left(\boldsymbol{\theta}_{w\pi_n}^* \right) \right| \right\} \leq B_2 < \infty$$

for $\mathbf{O} \in \mathcal{O}$ and $\pi_n \in \Pi_n$, where $\boldsymbol{\theta}_{w\pi_n}^*$ is the almost sure asymptotic limit of $\widehat{\boldsymbol{\theta}}_{w\pi_n}(\mathbf{L}_0)$. Define $B^* = \max(B_1, B_2)$, for any subgroup w , $\gamma_w = \Pr(\mathbf{L}_0 \in w)$, $n(w) = \sum_{i=1}^n I\{\mathbf{L}_{0,i} \in w\}$, $\widehat{\gamma}_w = n_w/n$, $\widehat{\boldsymbol{\theta}}_w$ as the nuisance parameters estimated using data from subgroup w , and $Y_{w,i}^*(\widehat{\boldsymbol{\theta}}_w)$ as the associated transformed outcome. Assumption B.1 and equation (18) in Nobel [1996] imply

$$\begin{aligned} & \int_{\mathcal{L}_0} |\widehat{r}_n(\mathbf{l}_0) - \widetilde{r}_n(\mathbf{l}_0)|^2 dP(\mathbf{l}_0) \\ & \leq 2B^* \sum_{w \in \widehat{\psi}_n} \gamma_w \left| \frac{1}{n(w)} \sum_{i=1}^n I\{\mathbf{L}_{0,i} \in w\} \{Y_{w,i}^*(\widehat{\boldsymbol{\theta}}_w) - r(\mathbf{L}_{0,i})\} \right| \\ & \leq 2B^* \sum_{w \in \widehat{\psi}_n} \widehat{\gamma}_w \left| \frac{1}{n(w)} \sum_{i=1}^n I\{\mathbf{L}_{0,i} \in w\} \{Y_{w,i}^*(\widehat{\boldsymbol{\theta}}_w) - r(\mathbf{L}_{0,i})\} \right| \\ & \quad + 2B^* \sum_{w \in \widehat{\psi}_n} \left| \frac{1}{n(w)} \sum_{i=1}^n I\{\mathbf{L}_{0,i} \in w\} \{Y_{w,i}^*(\widehat{\boldsymbol{\theta}}_w) - r(\mathbf{L}_{0,i})\} \right| |\widehat{\gamma}_w - \gamma_w| \\ & \leq 2B^* \sup_{\pi_n \in \Pi_n} \sum_{w \in \pi_n} \widehat{\gamma}_w \left| \frac{1}{n(w)} \sum_{i=1}^n I\{\mathbf{L}_{0,i} \in w\} \{Y_{w,i}^*(\widehat{\boldsymbol{\theta}}_w) - r(\mathbf{L}_{0,i})\} \right| \\ & \quad + 4B^{*2} \sup_{\pi_n \in \Pi_n} \sum_{w \in \pi_n} |\widehat{\gamma}_w - \gamma_w|. \end{aligned}$$

Applying Proposition 2, Lemma 3, and Theorem 7 in Nobel [1996] with assumption B.2 gives

$\sup_{\pi_n \in \Pi_n} \sum_{w \in \pi_n} |\widehat{\gamma}_w - \gamma_w| = o_P(1)$. Hence,

$$\int_{\mathcal{L}_0} |\widehat{r}_n(\mathbf{l}_0) - \widetilde{r}_n(\mathbf{l}_0)|^2 dP(\mathbf{l}_0) \leq 2B_1^* \sup_{\pi_n \in \Pi_n} \sum_{w \in \pi_n} \left| \frac{1}{n} \sum_{i=1}^n I\{\mathbf{L}_{0,i} \in w\} \{Y_{w,i}^*(\widehat{\boldsymbol{\theta}}_w) - r(\mathbf{L}_{0,i})\} \right| + o_P(1).$$

Using Taylor series arguments and assumption B.3 gives

$$\begin{aligned}
& \int_{\mathcal{L}_0} |\widehat{r}_n(\mathbf{l}_0) - \widetilde{r}_n(\mathbf{l}_0)|^2 dP(\mathbf{l}_0) \\
& \leq 2B^* \sup_{\pi_n \in \Pi_n} \sum_{w \in \pi_n} \left| \frac{1}{n} \sum_{i=1}^n I(\mathbf{L}_{0,i} \in w) \left\{ Y_{w,i}^*(\boldsymbol{\theta}_w^*) + (\widehat{\boldsymbol{\theta}}_w - \boldsymbol{\theta}_w^*) \frac{\partial Y_{w,i}^*(\boldsymbol{\theta})}{\partial \boldsymbol{\theta}} \Big|_{\boldsymbol{\theta}=\boldsymbol{\theta}_w^*} - r(\mathbf{L}_{0,i}) \right\} \right| + o_P(1) \\
& \leq 2B^* \sup_{\pi_n \in \Pi_n} \sum_{w \in \pi_n} \left| \frac{1}{n} \sum_{i=1}^n I(\mathbf{L}_{0,i} \in w) \{Y_{w,i}^*(\boldsymbol{\theta}_w^*) - r(\mathbf{L}_{0,i})\} \right| + o_P(1),
\end{aligned}$$

where the last equality follows as $\boldsymbol{\theta}_w^*$ is defined as the asymptotic limit of $\widehat{\boldsymbol{\theta}}_w$.

The same steps as in the proof of Theorem A.6.4 in [Yang et al. \[2022\]](#) give

$$2B^* \sup_{\pi_n \in \Pi_n} \sum_{w \in \pi_n} \left| \frac{1}{n} \sum_{i=1}^n I(\mathbf{L}_{0,i} \in w) \{Y_{w,i}^*(\boldsymbol{\theta}_w^*) - r(\mathbf{L}_{0,i})\} \right| = o_P(1).$$

Combining the above gives

$$\int_{\mathcal{L}_0} |\widehat{r}_n(\mathbf{l}_0) - \widetilde{r}_n(\mathbf{l}_0)|^2 dP(\mathbf{l}_0) = o_P(1).$$

The Proof of Theorem 1 in [Nobel \[1996\]](#) shows that

$$\int_{\mathcal{X}} |r(\mathbf{l}_0) - \widetilde{r}_n(\mathbf{l}_0)|^2 dP(\mathbf{l}_0) = o_P(1).$$

Combining all of the above gives the desired result

$$\int_{\mathcal{L}_0} |r(\mathbf{l}_0) - \widehat{r}_n(\mathbf{l}_0)|^2 dP(\mathbf{l}_0) = o_P(1).$$

Appendix C Simulations

We conducted simulations to evaluate the finite sample performance of the SDDL algorithm.

C.1 Data generation

The baseline covariate vector \mathbf{L}_0 was simulated from a five-dimensional mean zero multivariate normal distribution where diagonal elements of the variance matrix were all equal to 1 and all off-diagonal elements were equal to 0.2. The baseline treatment indicator A_0 was simulated from a Bernoulli distribution with parameter

$$\Pr(A_0 = 1 | \mathbf{L}_0) = \text{expit} \left[-0.5 + 0.2L_0^{(1)} + 0.2L_0^{(2)} + 0.4L_0^{(3)} + 0.5L_0^{(4)} \right],$$

where $\text{expit}(x) = \exp(x)/(1 + \exp(x))$. The baseline censoring indicator $C_0^{a_0}$ was simulated from a Bernoulli distribution with parameter

$$\Pr(C_0^{a_0} = 1 | \mathbf{L}_0) = \text{expit} \left[-4 + 0.8a_0 + 0.3L_0^{(1)} - 0.3L_0^{(2)} - 0.3L_0^{(3)} + 0.1L_0^{(4)} \right].$$

The covariate vector at time one had three elements $\mathbf{L}_1 = (Y_1, L_1^{(1)}, L_1^{(2)})$. All of $Y_1^{a_0, c_0=0}$, $L_1^{(1), a_0, c_0=0}$ and $L_1^{(2), a_0, c_0=0}$ are normally distributed with means

$$\begin{aligned} \mathbb{E} \left[Y_1^{a_0, c_0=0} | \mathbf{L}_0 \right] &= -3 + 0.1a_0 + 0.3L_0^{(1)} - 2a_0 I \left[L_0^{(2)} > 0.5 \right] + 2L_0^{(4)} + 2L_0^{(5)}, \\ \mathbb{E} \left[L_1^{(1), a_0, c_0=0} | \mathbf{L}_0 \right] &= 0.2a_0 + 0.5L_0^{(1)} - 0.4L_0^{(2)} - 0.4L_0^{(3)} + 0.5L_0^{(4)} - 0.5L_0^{(5)}, \\ \mathbb{E} \left[L_1^{(2), a_0, c_0=0} | \mathbf{L}_0, L_1^{(1), a_0, c_0=0} \right] &= 0.1a_0 + 0.1L_0^{(1)} + 0.1L_0^{(2)} - 0.4L_0^{(3)} + 0.5L_1^{(1), a_0, c_0=0} - 0.5L_0^{(5)}. \end{aligned}$$

The variance of $Y_1^{a_0, c_0=0}$ is 1, and the variance of $L_1^{(1), a_0, c_0=0}$ and $L_1^{(2), a_0, c_0=0}$ are both 0.4 and the off-diagonal elements of the variance matrix for \mathbf{L}_1 are all zero.

The treatment at time one follows a Bernoulli distribution with parameter

$$\begin{aligned} &\Pr \left[A_1^{a_0, c_0=0} = 1 | \mathbf{L}_0, \mathbf{L}_1^{a_0, c_0=0} \right] \\ &= \text{expit} \left[-1 + 0.1L_0^{(1)} + 0.1L_0^{(2)} + 0.2L_0^{(3)} + 0.2L_0^{(4)} - L_1^{(1), a_0, c_0=0} - 0.5L_1^{(2), a_0, c_0=0} \right]. \end{aligned}$$

The censoring indicator at time 1 follows a Bernoulli distribution with parameter

$$\begin{aligned} & \Pr \left[C_1^{\mathbf{a}, c=0} = 1 \mid \mathbf{L}_0, \mathbf{L}_1^{a_0, c_0=0} \right] \\ & = \text{expit} \left[-4 + 0.3a_0 + 0.5a_1 + 0.3L_0^{(1)} - 0.3L_0^{(2)} - 0.3L_0^{(3)} + 0.1L_1^{(1), a_0, c_0=0} + 0.1L_0^{(5)} \right]. \end{aligned}$$

The outcome $Y_2^{\mathbf{a}, c=0}$ follows a normal distribution with mean

$$\begin{aligned} \mathbb{E} \left[Y_2^{\mathbf{a}, c=0} \mid \mathbf{L}_0, \mathbf{L}_1^{a_0, c_0=0} \right] & = -2 + 0.1a_0 + 0.1a_1 + 0.3L_0^{(1)} - 2a_0I(L_0^{(2)} > 0.5) - 2a_1I(L_0^{(2)} > 0.5) \\ & \quad - 0.3L_0^{(3)} + 2L_1^{(1), a_0, c_0=0} + 2L_1^{(2), a_0, c_0=0} \end{aligned}$$

and variance 1. We simulated 12,000 observations and randomly split the dataset into an initial tree building dataset consisting of 10,000 observations and a final tree selection dataset which consisted of the remaining 2,000 observations. We focused on contrasting treatment regimes $\mathbf{a}_1 = \mathbf{1} = (1, 1)$ and $\mathbf{a}_0 = \mathbf{0} = (0, 0)$. For this data generating distribution the treatment effect differs depending on whether $L_0^{(2)} > 0.5$ or not and the correct tree splits on $L_0^{(2)}$ at split-point 0.5.

When estimating the models for the probability of treatment assignment, the probability of dropping out of the study, and the model for the expectation of the pseudo-outcome at each time, we used generalized linear regression models with linear and additive main effects for all past covariate and treatment variables. We used 1,000 simulations to evaluate the performance of the SDLD algorithm.

To evaluate the algorithm we used the following evaluation measures:

- Proportion of correct trees: We say a tree is correct if it splits the correct number of times on each variable [Steingrímsson et al., 2016]. In our setup this means splitting once on $L_0^{(2)}$ and never on other variables.
- The number of terminal nodes in the tree.
- The number of noise variables that are split on (i.e., variables which are not treatment effect modifiers).

- Proportion of times the first split in the initial tree is on $L_0^{(2)}$.
- Pairwise prediction similarity [Steingrímsson et al., 2016]: Pairwise prediction similarity measures the ability of the SDDL algorithm to stratify observations into correct groups and is defined as $1 - \frac{\sum_{i=1}^{1000} \sum_{j>1}^{1000} \frac{|I_T(i,j) - I_M(i,j)|}{\binom{1000}{2}}}{\binom{1000}{2}}$, where $I_T(i, j)$ and $I_M(i, j)$ are indicators for whether individuals i and j fall in the same terminal node running down the correct tree and the estimated tree, respectively. The pairwise prediction similarity is bounded between zero and one with higher values indicating better performance.

C.2 Simulation Results

The SDDL algorithm identified the correct tree in 89.5% of the simulation runs and the pairwise prediction similarity was 0.98. The average size of the tree was 2.2, which is close to the size of the correct tree, 2. The average number of noise variables the tree splits on was 0.16. The initial tree built by the initial tree building step first splits on $L_0^{(2)}$ (i.e., the correct covariate we expect the tree to first split on) in all simulation runs.

Appendix D Additional information for the analysis of the AM-PATH data

In this section we provide additional details on the analysis in Section 4. For the analysis all continuous variables were standardized.

Definition of treatment: When defining treatment assignment in each time period, we focused on visits where either a) an individual was assigned to at least three medications [World Health Organization, 2016] or b) an individual was assigned to less than three medications and one of them was DTG. We defined treatment status as being on DTG ($A_k=1$) if the individual was on DTG at the last visit in the time period and not being on DTG ($A_k=0$) if the individual was not on DTG at the last visit in the time period. Treatment assignment was considered missing if there was no visit within a time period with available treatment information that satisfies either conditions a) or b) listed above.

Definition of outcome and time-varying covariates: To define the values of time-varying covariates in each time period (including the value of the outcome) we used data from the last visit before or at the visit where treatment was captured if there was no switch of DTG status in the time period and before or at the last visit when a switch happened if there was switch of DTG status in the time period. If treatment was missing in the time period, we used the last observed value of time-varying covariates in the time period. In the last time period ($K + 1$), we used the last observed outcome measure as Y_{K+1} . If there were no observed measurements satisfying the aforementioned condition, outcome and/or time-varying covariates were considered missing in the time period.

If outcome or treatment information was not available at time 0, we re-defined day 0 as the date of the first visit. If weight was still missing at time 0 after re-defining day 0, we further re-defined day 0 as the date of the visit with the first weight measurement. If treatment was still missing at time 0 after re-defining day 0, we move the date of visit with the first observed treatment to the last day of time 0 (i.e., day $d - 1$ for a window length of d days); therefore, day 0 was re-defined as $(d - 1)$ days before date of visit with the first observed treatment. After time 0 we used carry-over from the previous time periods to handle missing outcome and treatment information. We excluded participants who still had missing values in outcome and treatment at time 0 after being pre-processed as described above. That is, we excluded participants with 1) no observed weight measurements, 2) no observed treatment, or 3) no observed treatment after the first observed weight measurement.

To handle missingness in viral load, we created an ordinal variable with missingness as the lowest category. The new variable had four categories ordered as 1) missing, 2) $[0, 10^3)$, 3) $[10^3, 10^4)$, and 4) $[10^4, \infty)$. In the analysis, we dropped all covariates that had more than 10% missing values. For the remaining time-varying covariates (most with $\leq 1.5\%$ missing data), we handled missing data by carrying over values from the previous time period if there were observed measurements to carry over; otherwise for continuous covariates, we imputed the missing values using the average of the observed values in the time period, and for binary covariates, we imputed the missing values by 0. Tables 1 and 2 show the number and proportion of missing values in covariates that were

dropped and in time-varying covariates that were used, respectively. Table 3 present the summary for each covariate used in the analysis before and after imputation and the two distributions are very similar.

Covariate Uncensored individuals	Visit 0 (%) $n = 84,445$	Visit 1 (%) $n = 71,431$	Visit 2 (%) $n = 64,353$	Visit 3 (%) $n = 58,646$
Employed outside home	31,807 (37.7%)	-	-	-
Electricity in home	31,669 (37.5%)	-	-	-
Water piped in home	31,928 (37.8%)	-	-	-
CD4 count	77,760 (92.1%)	66,453 (93.0%)	60,252 (93.6%)	55,306 (94.3%)
Blood glucose	84,407 (> 99.9%)	71,376 (99.9%)	64,300 (99.9%)	58,582 (99.9%)
Fasting serum glucose	84,438 (> 99.9%)	71,420 (> 99.9%)	64,338 (> 99.9%)	58,628 (> 99.9%)

Table 1: Number and proportion of missing values in covariates that were dropped from the analysis.

Covariate Uncensored individuals	Visit 0 $n = 84,445$	Visit 1 $n = 71,431$	Visit 2 $n = 64,353$	Visit 3 $n = 58,646$
Systolic blood pressure	1,269 (1.5%)	179 (0.3%)	66 (0.1%)	35 (0.1%)
Diastolic blood pressure	1,276 (1.5%)	181 (0.3%)	68 (0.1%)	36 (0.1%)
Height	4,276 (5.1%)	1,659 (2.3%)	862 (1.3%)	405 (0.7%)
TB treatment	56 (0.1%)	11 (0%)	4 (0%)	3 (0%)
Married/living with partner	3,019 (3.6%)	484 (0.7%)	174 (0.3%)	71 (0.1%)
Covered by NHIF	6,362 (7.5%)	2,305 (3.2%)	1,039 (1.6%)	496 (0.8%)

Table 2: Number of proportion of missing values in time-varying covariates that were used in the analysis. TB refers to tuberculosis; NHIF refers to National Health Insurance Fund.

Table 4 shows the estimated average weight had all individuals been always and never on DTG-containing ARTs and the average weight gain when comparing always being on DTG-containing ARTs to never being on DTG-containing ARTs supporting Figure 1. The confidence intervals are estimated using the non-parametric bootstrap with 10,000 bootstrap samples.

Figure 3 plots the estimated average weight gain from receiving DTG-containing ART at each time for the subgroups discovered by the SDDL algorithm. The left panel shows the average effect among males and females and the right panel shows the average effect among females younger and older than or equal to 42.8 years old. The results show that both males and females gain most weight in the first 200 days; there is almost no additional weight gain after the first 200 days for males and there is a slight increase in weight gain from being on DTG-containing ART for a longer period of time among females. There is a large overlap of the confidence intervals for weight gain among younger and older females.

Covariates	L_0 ($n = 84,445$)		L_1 ($n = 71,431$)	
	Before	After	Before	After
Male, $n(\%)$	28,440 (33.7%)		-	
Age when starting ART, years	38.1 ± 10.4		-	
Age at visit 0, years	42.1 ± 11.0		-	
Time on ART at time 0, years	4.0 ± 3.9		-	
Whether enrolled on or after July 1, 2016, $n(\%)$	24,688 (29.2%)		-	
Weight, kg	62.2 ± 12.5		-	
Viral load, $n(\%)$				
Missing	48,309 (57.2%)		10,043 (14.1%)	
$[0, 10^3)$	30,025 (35.6%)		54,954 (76.9%)	
$[10^3, 10^4)$	3,166 (3.7%)		3,459 (4.8%)	
$[10^4, \infty)$	2,945 (3.5%)		2,975 (4.2%)	
Systolic blood pressure, mmHg	118.9 ± 18.7	118.9 ± 18.6	119.8 ± 18.9	119.8 ± 18.9
Diastolic blood pressure, mmHg	73.9 ± 12.1	73.9 ± 12.0	73.9 ± 12.3	73.9 ± 12.2
Height, cm	165.7 ± 9.2	165.7 ± 9.0	165.6 ± 9.5	165.6 ± 9.3
Active TB, $n(\%)$	2,821 (3.3%)		2,479 (3.5%)	
TB treatment, $n(\%)$	1,936 (2.3%)	1,936 (2.3%)	596 (0.8%)	596 (0.8%)
Married/living with partner, $n(\%)$	47,759 (58.7%)	47,759 (56.6%)	41,065 (57.9%)	41,065 (57.5%)
Covered by NHIF, $n(\%)$	16,485 (21.1%)	16,485 (19.5%)	16,104 (23.3%)	16,104 (22.5%)
	L_2 ($n = 64,353$)		L_3 ($n = 58,646$)	
	Before	After	Before	After
Viral load, $n(\%)$				
Missing	4,622 (7.2%)		2,368 (4.0%)	
$[0, 10^3)$	54,117 (84.1%)		51,749 (88.2%)	
$[10^3, 10^4)$	3,269 (5.1%)		2,797 (4.8%)	
$[10^4, \infty)$	2,345 (3.6%)		1,732 (3.0%)	
Systolic blood pressure, mmHg	120.6 ± 18.9	120.6 ± 18.9	121.2 ± 18.8	121.2 ± 18.8
Diastolic blood pressure, mmHg	74.6 ± 12.1	74.6 ± 12.1	75.1 ± 12.1	75.1 ± 12.1
Height, cm	165.7 ± 9.3	165.7 ± 9.2	165.8 ± 9.0	165.8 ± 9.0
Active TB, $n(\%)$	2,349 (3.7%)		2,167 (3.7%)	
TB treatment, $n(\%)$	369 (0.6%)	369 (0.6%)	277 (0.5%)	277 (0.5%)
Married/living with partner, $n(\%)$	37,061 (57.7%)	37,061 (57.6%)	33,164 (56.6%)	33,164 (56.5%)
Covered by NHIF, $n(\%)$	15,970 (25.2%)	15,970 (24.8%)	15,779 (27.1%)	15,779 (26.9%)

Table 3: Summary of covariates used in the analysis before and after imputation. For binary or ordinal covariates, we present the number and proportion of participants falling in the listed category; for continuous covariates, we present the mean and standard deviation. For covariates with no missing values, we present one summary for before and after imputation. ART refers to antiretroviral therapy; TB refers to tuberculosis; NHIF refers to National Health Insurance Fund.

Time	Uncensored	Always DTG		Never DTG		DTG Effect
k	n	n	$\hat{E} \left[Y_k^{\bar{1}_{k-1}, \bar{c}_{k-1}=0} \right]$	n	$\hat{E} \left[Y_k^{\bar{0}_{k-1}, \bar{c}_{k-1}=0} \right]$	
1	71,431	5,700	63.27 (63.05, 63.49)	65,731	62.18 (62.09, 62.27)	1.09 (0.88, 1.30)
2	64,353	3,083	63.81 (63.56, 64.06)	59,550	62.60 (62.51, 62.70)	1.20 (0.96, 1.44)
3	58,646	1,350	64.10 (63.79, 64.41)	53,164	62.83 (62.73, 62.92)	1.28 (0.96, 1.59)
4	54,005	517	64.59 (64.17, 65.00)	44,473	63.18 (63.08, 63.28)	1.41 (0.99, 1.82)

Table 4: The table shows results from analysis of the whole analysis set. The table shows the total number of individuals with data available at each time k and the number of individuals that were always or never on DTG-containing ART up to that time. The column labeled $\hat{E} \left[Y_k^{\bar{1}_{k-1}, \bar{c}_{k-1}=0} \right]$ shows the estimated weight (kg) using targeted maximum likelihood estimation (TMLE) if always on DTG-containing ARTs and the column labeled $\hat{E} \left[Y_k^{\bar{0}_{k-1}, \bar{c}_{k-1}=0} \right]$ shows the estimated weight if never on DTG-containing ARTs. The column labeled DTG Effect shows the estimated causal effect of always vs. never being on a DTG-containing ART on weight gain since time 0.

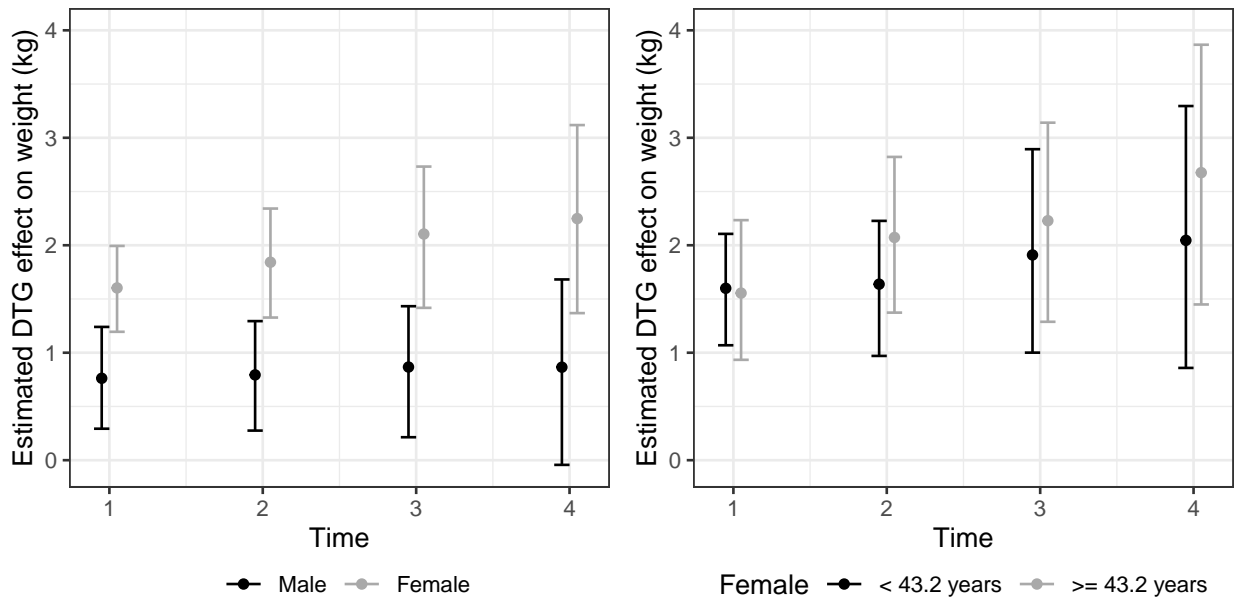


Figure 3: Estimated causal effect at each time on average weight in the subgroups discovered by the SDDL algorithm comparing always vs. never being on a DTG-containing ART. The left panel shows the average effect among males and females and the right panel shows the average effect among females who are younger and older than or equal to 42.8 years old.

Stability of the SDDL algorithm: Table 5 presents the number of subgroups having differential effects of DTG-containing ARTs on weight gain discovered by the SDDL algorithms for 1,000 different data-splits. Table 6 presents the number of times the final trees make splits on the variables in \mathbf{L}_0 across different splits of the data.

Subgroups	1	2	3	4
n	245	206	322	227

Table 5: Number of subgroups discovered by the SDDL algorithm across different data-splits

Covariate	First split	Other splits	Total
Male	482	61	543
Age when starting ART	66	90	156
Age at time 0	64	264	328
Time on ART at time 0	13	2	15
Whether enrolled on or after July 1, 2016	11	0	11
Weight	14	138	152
Viral load	3	46	49
Systolic blood pressure	12	58	70
Diastolic blood pressure	9	34	43
Height	69	56	125
Active TB	0	0	0
TB treatment	0	0	0
Married/living with partner	12	25	37
Covered by NHIF	0	2	2

Table 6: Number of times the final tree splits on each variables in \mathbf{L}_0 across the 1000 different data splits. ART refers to antiretroviral therapy; TB refers to tuberculosis; NHIF refers to National Health Insurance Fund.